Letter

Two-particle Berry phase mechanism for Dirac and Majorana Kramers pairs of corner modes

Yi Tan,[1,2,*] Zhi-Hao Huang,[1,2,*] and Xiong-Jun Liu[1,2,3,4,†]

[1]*International Center for Quantum Materials and School of Physics, Peking University, Beijing 100871, China*

[2]*Collaborative Innovation Center of Quantum Matter, Beijing 100871, China*

[3]*CAS Center for Excellence in Topological Quantum Computation, University of Chinese Academy of Sciences, Beijing 100190, China*

[4]*Institute for Quantum Science and Engineering and Department of Physics, Southern University of Science and Technology, Shenzhen 518055, China*

(Received 6 July 2021; accepted 5 January 2022; published 13 January 2022)

We uncover an alternative two-particle Berry phase mechanism to realize exotic corner modes in second-order topological insulators (TIs) and topological superconductors (TSCs) with time-reversal symmetry. We show that the nontrivial pseudospin textures of edge states in two different types of two-dimensional TIs give rise to different two-particle geometric phases in the particle-hole and particle-particle channels, respectively, for which the edge mass domain walls or intrinsic π junctions emerge across corners when an external magnetic field or s-wave superconductivity is considered, hosting Dirac or Majorana corner modes. Remarkably, with this mechanism we predict the Majorana Kramers pair of corner modes by directly coupling the edge of a type-II time-reversal invariant TI to a uniform s-wave SC, in sharp contrast to previous proposals which rely on unconventional SC pairing or a complex setting for a fine-tuned SC π junction. We find Au/GaAs(111) to be a realistic material candidate for realizing such a Majorana Kramers pair of corner modes.

DOI: 10.1103/PhysRevB.105.L041105

Introduction. Topological phases have generated great interest in the past decades [1–3]. Recently, higher-order topological insulators (TIs) and topological superconductors (TSCs) were proposed [4–10]. An nth-order TI (TSC) in d dimension (dD) features topologically protected gapless states on its $(d-n)$D boundary, but is gapped elsewhere. For example, a 2D second-order topological insulator (SOTI) hosts in-gap modes at the corners, while both its 2D bulk and 1D edges are gapped [11,12]. The physics of corner modes is readily understood from the perspective of Dirac equations: The original helical edge states of a 2D time-reversal (TR) invariant TI are gapped by a sign-changing Dirac mass, leading to the corner modes at the mass domain walls [13–15]. The same picture applies to the case of 2D second-order topological superconductors (SOTSCs).

While interest has grown rapidly in the higher-order topological phases, the experimental realization of such phases in solid materials is rare, although various interesting theoretical schemes have been proposed [8,11,12,16–23]. In comparison with higher-order topological insulators, realizing superconducting counterparts is usually even more difficult [24–32]. In particular, for second-order time-reversal (TR) invariant TSCs which host Majorana Kramers pairs (MKPs) of the corner modes, the existing proposals rely on either the coupling of TI helical edge states to unconventional superconductivity [33,34] or complex settings for fine-tuned SC π junctions [35–37]. The MKPs obey the symmetry-protected non-Abelian statistics, manifesting a new type of non-Abelian anyon [38–44]. Although currently very scarce, the search for experimental schemes to realize MKPs [45], is highly significant and of broad interest.

In this Letter, we propose a fundamental mechanism by introducing an alternative concept of a two-particle Berry phase to characterize and realize topological corner modes in second-order topological phases. We show that two different scenarios of Berry phases arise from the pseudospin textures of edge states [46] in two different types of 2D TIs, leading to sign changes in the gap that opens at the edge and across corners when an external magnetic field or superconductivity is applied. In the SOTI phase, the mass domain wall emerges and originates from the two-particle Berry phase of a particle-hole channel, leading to the transition from a quantum spin Hall (QSH) to SOTI phase by applying a uniform in-plane magnetic field. In the SOTSC phase, *intrinsic* π junctions emerge at the corners, resulting from the two-particle Berry phases of the particle-particle channel (Cooper pair), giving rise to MKPs of the corner modes with TR symmetry. Remarkably, with this mechanism we predict that the MKPs can be realized by directly superposing a type-II TI on a uniform s-wave SC, in sharp contrast to previous proposals [33–37]. This prediction updates a traditional viewpoint that, due to the TR symmetry, a uniform s-wave proximate SC can induce a uniform pairing order without a node in and thus fully gaps out the helical edge states of a TI (see, e.g., Refs. [47,48]). Our finding shows that for a broad class of the quantum spin Hall insulators, the intrinsic π junction emerges across the corners when the edge is coupled to a uniform s-wave SC, leading to MKPs of the corner modes. We show the QSH insulator Au/GaAs(111) thin film [49,50] is a 2D material candidate for the realization of MKPs, and further provide a generic guideline in the search for such SOTSC phases.

*These authors contributed equally to this work.

†Corresponding author: xiongjunliu@pku.edu.cn.

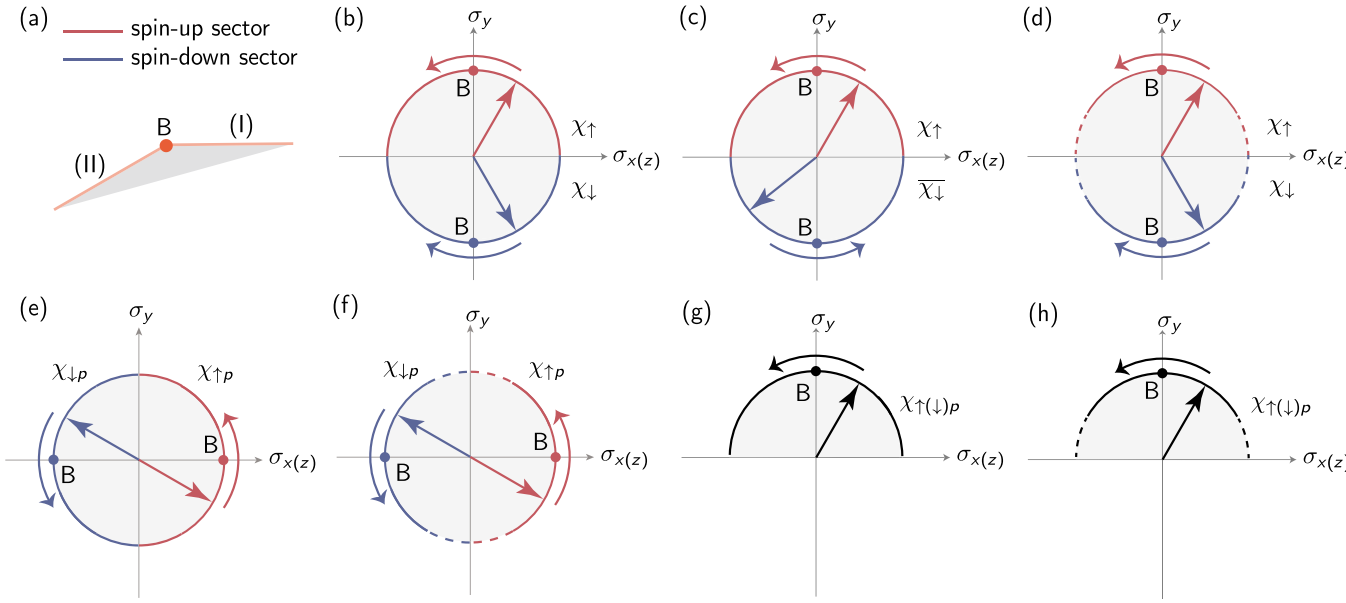

FIG. 1. Boundary pseudospin textures of TIs crossing corner B. (a) Schematic plot of the adjacent edges in real space. (b) Pseudospin trajectories for $|\chi_\uparrow\rangle$ (red solid lines) and $|\chi_\downarrow\rangle$ (blue solid lines) wind oppositely in intrinsic space. The straight red (blue) arrows denote the pseudospin vectors for $|\chi_\uparrow\rangle$ ($|\chi_\downarrow\rangle$). (c) The joint trajectory for $|\chi_\uparrow\rangle$ and $\overline{|\chi_\downarrow\rangle}$ can be viewed as a closed loop in intrinsic space, which enables a well-defined two-state Berry phase in the PH channel γ_{ph}, leading to the Dirac corner modes. (d) The conclusion in (c) also applies to the situation where pseudospin trajectories are nonclosed and can be connected by the continuation trajectories (dashed lines). (e) and (g) The winding of pseudospin trajectories within both spin sectors is in the same direction. The straight black arrows represent the coinciding of pseudospin vectors for $|\chi_\uparrow\rangle$ and $|\chi_\downarrow\rangle$.The two-state Berry phase in the PP channel γ_{pp} is of importance since the joint trajectories for $|\chi_{\uparrow p}\rangle$ and $|\chi_{\downarrow p}\rangle$ are closed, guaranteeing the appearance of MKPs. This result can be extended to nonclosed cases (f) and (h).

The generic edge theory. We start with a generic edge theory of the geometric phase mechanism for the corner modes. The theory is extended from a previous result that the chiral edge state in a class of quantum anomalous Hall (QAH) insulators exhibits topological (pseudo)spin texture in real space, with the pseudospin polarization of each edge state winding one big circle along the closed 1D boundary in the presence of chiral symmetry [46,51]. Such a pseudospin texture defines a π-Berry phase on the boundary. For a TR invariant TI formed by two copies of QAH insulators with opposite Chern numbers, its helical edge states form Kramers pairs of the time-reversal symmetry (TRS) $\mathcal{T} = is_y\mathcal{K}$, with s_y being the spin operator and $\mathcal{K}$ the complex conjugate. The pseudospin polarizations of spin-up ($|\chi_\uparrow\rangle$) and spin-down ($|\chi_\downarrow\rangle$) edge states are given by $\langle\boldsymbol{\sigma}_\uparrow\rangle = \langle\chi_\uparrow|s_0\boldsymbol{\sigma}|\chi_\uparrow\rangle$ and $\langle\boldsymbol{\sigma}_\downarrow\rangle = \langle\chi_\downarrow|s_0\boldsymbol{\sigma}|\chi_\downarrow\rangle$, where the pseudospin operators $\boldsymbol{\sigma}$ denote the orbital (or sublattice) degree of freedom. When traveling from one edge to a neighboring edge across a corner point B in real space [Fig. 1(a)], the pseudospin direction ($\langle\boldsymbol{\sigma}_{\uparrow,\downarrow}\rangle$) of a single state in general does not trace a closed loop. However, a *two-state Berry phase* can be defined when the pseudospin polarizations are inverted across the corner for both spin-up and spin-down sectors. Two basic cases corresponding to two fundamental types of TIs are of particular interest and are studied below.

First, the pseudospin trajectories of the two spin sectors wind oppositely, e.g., $(\langle\sigma_{\uparrow x}\rangle, \langle\sigma_{\uparrow y}\rangle) = (\langle\sigma_{\downarrow x}\rangle, -\langle\sigma_{\downarrow y}\rangle)$ [Fig. 1(b)], so the joint pseudospin trajectory of the spin-up particle and spin-down hole is closed in intrinsic space [Fig. 1(c)]. The case where TR symmetry reverses only real spin but not pseudospin bases belongs to this scenario. We define the two-state Berry phase in the particle-hole (PH) channel as

$$\gamma_{ph} = \int_{\theta^{(\mathrm{I})}}^{\theta^{(\mathrm{II})}} d\theta \langle\chi_\uparrow(\theta)| \otimes \overline{\langle\chi_\downarrow(\theta)|}(-i\partial_\theta)|\chi_\uparrow(\theta)\rangle \otimes \overline{|\chi_\downarrow(\theta)\rangle}. \tag{1}$$

Here, $\theta^{(\mathrm{I,II})}$ stands for the normal direction of edge I and II, and the spin-down hole state $\overline{|\chi_\downarrow\rangle}$ is obtained by charge conjugation $\mathcal{K}$ on $|\chi_\downarrow\rangle$, equivalent to flipping a ket into a bra state. Applying a uniform in-plane Zeeman field $(\mathbf{M}\cdot\mathbf{s})\sigma_0$ breaks the TRS and introduces the mass term $\mathcal{H}_{\mathrm{mass}}$ [52] to the edge Dirac Hamiltonian $\mathcal{H}_{\mathrm{edge}} = vk_\parallel s_z$ [12]. The matrix element $\langle\chi_\uparrow|(\mathbf{M}\cdot\mathbf{s})\sigma_0|\chi_\downarrow\rangle$ resembles a particle-hole excitation gap on the edge, and when turning from edge I to edge II across the corner point B, the mass term is related by [52]

$$\langle\chi_\uparrow^{(\mathrm{II})}|(\mathbf{M}\cdot\mathbf{s})\sigma_0|\chi_\downarrow^{(\mathrm{II})}\rangle = e^{-i\gamma_{ph}}\langle\chi_\uparrow^{(\mathrm{I})}|(\mathbf{M}\cdot\mathbf{s})\sigma_0|\chi_\downarrow^{(\mathrm{I})}\rangle. \tag{2}$$

Consequently, for $\gamma_{ph} = \pm\pi$ a mass domain wall is obtained across the corner, giving zero-energy corner modes. This result can be extended to the more generic configuration where the pseudospin polarization of each spin sector is not fully inverted across the corner [Fig. 1(d)]. In this case we consider a continuation [shown in the dashed line of Fig. 1(d)] to connect them so that the two-state pseudospin trajectory is still closed and a two-state π-Berry phase results. As long as no node of mass is obtained on the continuation trajectories, the mass domain wall must be obtained across the corner. We note that the π-Berry phase and zero-energy mode for the insulating phase necessitate protection by a chiral-like symmetry [52], which anticommutes with all terms in the

Hamiltonian. When this symmetry is broken, the pseudospin texture will not be fully in plane and the Berry phase is no longer strictly quantized to π (even with closed pseudospin trajectories via continuation), hence not guaranteeing a full sign reversion of the edge mass term. In this case the corner mode has finite energy but may still be within the gap if the Berry phase is close to the π value.

The second even more nontrivial case that we unveil is the two-state Berry phase in the particle-particle (PP) channel, which corresponds to realizing MKPs of the corner modes in SOTSCs when the edge is proximately coupled to a uniform s-wave SC. The case that TR symmetry reverses both real spin and pseudospin bases belongs to this scenario. Particularly, when the pseudospins of both spin sectors wind in the same direction across the corner, e.g., $(\langle\sigma_{\uparrow x}\rangle, \langle\sigma_{\uparrow y}\rangle) = \pm(\langle\sigma_{\downarrow x}\rangle, \langle\sigma_{\downarrow y}\rangle)$ [Figs. 1(e) and 1(g)], the two-state Berry phase in the PH channel vanishes, but is nontrivial in the PP channel,

$$\gamma_{pp} = \int_{\theta^{(\mathrm{I})}}^{\theta^{(\mathrm{II})}} d\theta \langle\chi_{\uparrow p}(\theta)| \otimes \langle\chi_{\downarrow p}(\theta)| \times (-i\partial_\theta)|\chi_{\uparrow p}(\theta)\rangle \otimes |\chi_{\downarrow p}(\theta)\rangle. \quad (3)$$

For the edge Hamiltonian $\mathcal{H}_{\mathrm{edge}} = ivk_\parallel \tau_y s_z$, the SC pairing term induced in the edge states reads $\mathcal{H}_{\mathrm{mass}} = \langle\chi_{\uparrow p}|\Delta_s \tau_y s_y \sigma_0|\chi_{\downarrow h}\rangle \tau_y s_y$, where τ_y represents the particle-hole degree of freedom, and subscript p/h denotes the Nambu particle/hole sector. This matrix element gives the SC gap function in the edge and obeys [52]

$$\left\langle\chi_{\uparrow p}^{(\mathrm{II})}\middle|\Delta_s \tau_y s_y \sigma_0\middle|\chi_{\downarrow h}^{(\mathrm{II})}\right\rangle = e^{-i\gamma_{pp}}\left\langle\chi_{\uparrow p}^{(\mathrm{I})}\middle|\Delta_s \tau_y s_y \sigma_0\middle|\chi_{\downarrow h}^{(\mathrm{I})}\right\rangle. \quad (4)$$

In this case, a mass domain wall (an *intrinsic* π junction) is obtained when $\gamma_{pp} = \pm\pi$ and harbors at each corner a MKP, which obeys symmetry-protected non-Abelian statistics [38–44]. With the particle-hole symmetry being always present in superconductors, the MKPs of the zero corner modes are protected by time-reversal symmetry, without the necessity of a chiral-like symmetry in the insulators. We emphasize that in this realization we directly superpose TI on a uniform and conventional s-wave SC, in sharp contrast to previous proposals of realizing MKPs of the corner modes [33–37]. Again, this result does not require the pseudospin to be fully inverted across the corner, as long as no node exists for the pairing order on the auxiliary trajectories [dashed lines in Figs. 1(f) and 1(h)].

Application to SOTSCs. The edge two-particle Berry phase theory provides an intuitive principle to realize SOTIs and SOTSCs, while we leave the discussion on SOTIs based on the first type of TI to the Supplemental Material [52], and hereby focus on the more nontrivial prediction of MKPs of the corner modes. As required, we consider a generic type-II TI with two orbitals α and β transforming into each other under TRS, and propose two minimal-model realizations with such a TI proximately coupled to an s-wave SC. The Hamiltonian in the $\psi = (\psi_{\uparrow\alpha}, \psi_{\uparrow\beta}, \psi_{\downarrow\alpha}, \psi_{\downarrow\beta})^T$ basis is $H_{1(2)} = \int d\mathbf{k}\, \psi^\dagger(\mathbf{k}) \mathcal{H}_{\text{TI-1(2)}} \psi(\mathbf{k}) + H_{s\text{-wave}}$, with $H_{s\text{-wave}} = \sum_{\sigma=\alpha,\beta} \int d\mathbf{k}\, \Delta_s [\psi_{\uparrow\sigma}(\mathbf{k})\psi_{\downarrow\sigma}(-\mathbf{k}) + \text{H.c.}]$ being TR invariant, and the low-energy band Hamiltonian

$$\mathcal{H}_{\text{TI-1(2)}} = (m - t|\mathbf{k}|^2) s_z \sigma_z + vk_x s_{0(z)} \sigma_x + vk_y s_{0(z)} \sigma_y. \quad (5)$$

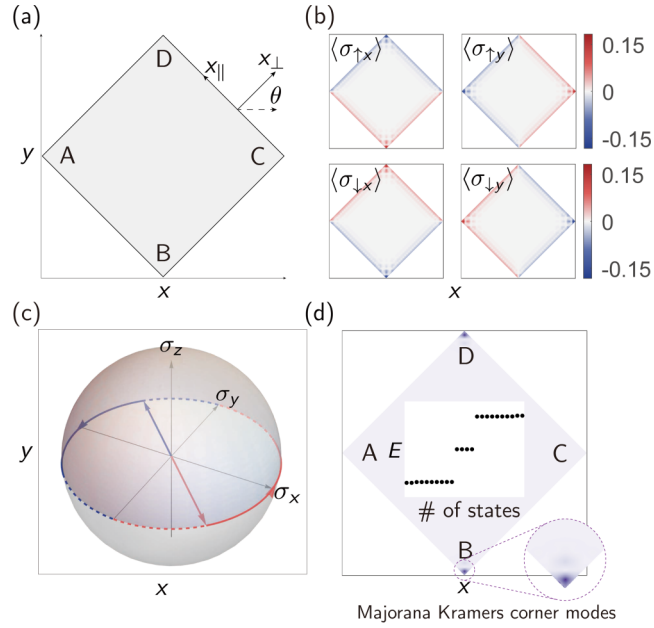

FIG. 2. Pseudospin analysis for the first minimal model, with parameters $m = 2$, $t = 1$, $v = 1$. (a) Illustration of the sample geometry and normal vector of edges. (b) Numerical results of the pseudospin polarizations of the two spin sectors. (c) Trajectories of pseudospin polarizations of spin-up particle (red solid line) and spin-down particle (blue solid line) states traveling from edge AB to BC, with valid continuation (dashed lines). Concatenating two trajectories gives a complete winding which encircles the 2π solid angle. (d) The distribution of the Dirac corner modes, and the energy level plotted under magnetic SC pairing strength $\Delta_s = 0.2$.

We consider a square-shape boundary, with the edges terminating the lattice in a tilted way [Fig. 2(a)]. When $\operatorname{sgn} m \operatorname{sgn} t > 0$, for an arbitrary sample edge with normal vector $\hat{\mathbf{x}}_\perp = (\cos\theta, \sin\theta)$, assuming a half-infinite sample area $x_\perp < 0$, we can solve out the helical edge states,

$$|\chi_\uparrow\rangle_{1,2} = \begin{bmatrix}1\\0\end{bmatrix}_s \otimes \begin{bmatrix}\frac{1}{\sqrt{2}}\\ -\frac{ie^{i\theta}}{\sqrt{2}}\end{bmatrix}_\sigma, \quad |\chi_\downarrow\rangle_{1,2} = \begin{bmatrix}0\\1\end{bmatrix}_s \otimes \begin{bmatrix}\frac{1}{\sqrt{2}}\\ \pm\frac{ie^{i\theta}}{\sqrt{2}}\end{bmatrix}_\sigma. \quad (6)$$

Thus the pseudospin polarizations for $|\chi_{\uparrow,\downarrow}\rangle$ are $\langle\boldsymbol{\sigma}_\uparrow\rangle_{1,2} = (\sin\theta, -\cos\theta, 0)$, $\langle\boldsymbol{\sigma}_\downarrow\rangle_{1,2} = (\mp\sin\theta, \pm\cos\theta, 0)$ [Fig. 2(b)]. We put here the numerical results for the first model, which is the case of the material candidate to be proposed later. The trajectories of two pseudospin polarizations across corner B (similar for other corners) are depicted as solid lines in Fig. 2(c), with in-between paths untraveled. So we can make a valid continuation [dashed lines in Fig. 2(c)] to concatenate the two trajectories, rendering a two-particle π-Berry phase in the PP channel. According to the generic theory, a mass domain wall arises at the corner on the real trajectories if applying an s-wave SC, as shown in the numerical results in Fig. 2(d). Note that the model has mirror symmetries. In particular, the mirror-x symmetry $\hat{M}_x = is_x\sigma_y\tau_z$ relates the edges AB and BC, forcing a SC π junction at intersection corner B, consistent with the Berry phase mechanism [52].

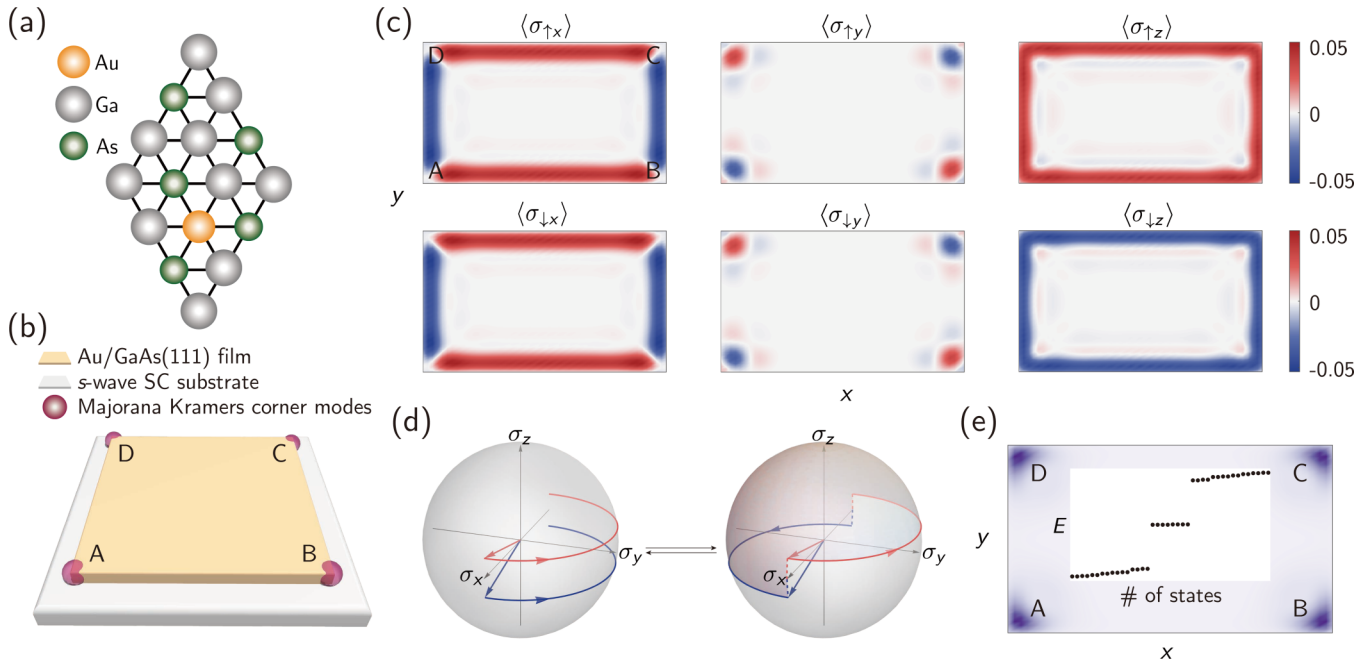

FIG. 3. The material realization of SOTSC and its pseudospin analysis. (a) $\sqrt{3}\times\sqrt{3}R30^\circ$ trigonal superlattice of Au/GaAs(111) surface. (b) Schematic plot of the QSH/s-wave SC heterostructure with MKPs of the corner modes. (c) Numerical results of the pseudospin polarizations. (d) Boundary pseudospin textures of the second type of QSH phase across corner B. Red and blue arcs are the real trajectories of pseudospin polarizations while dashed lines denote the continuation trajectories. (e) The distribution of MKPs and the energy levels. (c) and (e) are obtained with parameters $\varepsilon_s = 0.74$ eV, $\varepsilon_p = 0$ eV, $t_{ss\sigma} = -0.04$ eV, $t_{sp\sigma} = 0.04$ eV, $t_{pp\sigma} = 0.18$ eV, $t_{pp\pi} = 0.005$ eV, $\lambda = 0.06$ eV, $\mu = 0.555$ eV, $\Delta_s = 0.05$ eV.

Realistic materials. Now we propose the material realization of the above SOTSC. We focus on the Au/GaAs(111) thin film, which realizes a QSH phase in a triangular lattice [Fig. 3(a)] based on first-principles calculation [50]. The orbital components without SOC around the Γ point are described by the sp^2 basis $(s, p_x + ip_y, p_x - ip_y)$, which captures the minimal model of the system. With SOC, two types of QSH phases are supported, respectively corresponding to s-p band inversion (the first type) and p-p gap opening (the second type). In the following, we will study the second type of QSH phase, whose effective Hamiltonian is obtained by eliminating the bottom s orbital from the original sp^2 orbitals [50]. The Hamiltonian of the TI-SC heterostructure in the $\psi = (p_{\uparrow+}, p_{\uparrow-}, p_{\downarrow+}, p_{\downarrow-})^T$ basis is $H = \int d\mathbf{k}\, \psi^\dagger(\mathbf{k})\mathcal{H}_{\text{eff}}\psi(\mathbf{k}) + H_{s\text{-wave}}$, with $H_{s\text{-wave}} = \sum_{\sigma=+,-}\int d\mathbf{k}\, \Delta_s[p_{\uparrow\sigma}(\mathbf{k})p_{\downarrow\sigma}(-\mathbf{k}) + \text{H.c.}]$ and

$$\mathcal{H}_{\text{eff}}(\mathbf{k}) = a_0 s_0\sigma_0 + a_0'\left(k_x^2 + k_y^2\right)s_0\sigma_0 + \lambda s_z\sigma_z + a_x\left(k_x^2 - k_y^2\right)s_0\sigma_x + a_y k_x k_y s_0\sigma_y. \quad (7)$$

As required, here the TRS $\mathcal{T}'' = is_y\sigma_x\mathcal{K}$ reverses both spin and orbitals [52], and the necessary pseudospin texture in the generic theory is obtained. The pseudospin polarizations of an arbitrary edge read $\langle\boldsymbol{\sigma}_\uparrow\rangle = [a_\uparrow\cos 2\theta, a_\uparrow\sin 2\theta, (1-a_\uparrow^2)^{1/2}]$, $\langle\boldsymbol{\sigma}_\downarrow\rangle = [a_\downarrow\cos 2\theta, a_\downarrow\sin 2\theta, -(1-a_\downarrow^2)^{1/2}]$. It is easily verified that $a_\uparrow = a_\downarrow < 0$ [52], so the pseudospin texture turns out to satisfy $(\langle\sigma_{\uparrow x}\rangle, \langle\sigma_{\uparrow y}\rangle = \langle\sigma_{\downarrow x}\rangle, \langle\sigma_{\downarrow y}\rangle)$, which gives the two-particle Berry phase in the PP channel γ_{pp}. We further consider a rectangular sample proximate to the conventional s-wave SC [Fig. 3(b)]. When traveling across the corner B, the pseudospin trajectories [Fig. 3(c)] are depicted on the Bloch sphere [Fig. 3(d)]. The real trajectories of the pseudospin polarizations of $|\chi_{\uparrow p}\rangle$ (red semicircle) and $|\chi_{\downarrow p}\rangle$ (blue semicircle) can be connected by the continuation (dashed lines) with no nodes of pairing order existing in the continuation trajectories. Thus the two-particle π-Berry phase in the PP channel is obtained. Consequently, an intrinsic SC π junction results with a Majorana Kramers pair at the corner B, similar for the corners A, C, and D. The numerical results of MKPs and the energy spectrum [Fig. 3(e)] confirm our prediction. Also, an effective mirror symmetry $\hat{M}_{\hat{n}} = -i\tau_z s_z\sigma_z$ ($\hat{n} = \frac{\sqrt{2}}{2}\hat{x} + \frac{\sqrt{2}}{2}\hat{y}$) of the low-energy Hamiltonian can relate all adjacent edges, forcing the emergence of SC π junctions on every corner [52].

We note that our theory provides a generic guideline in the search for realistic materials of SOTSCs with MKPs via a uniform s-wave pairing and second type of TIs. In particular, in the type-II TI system the TRS reverses both the spin part and the orbital degree of freedom. Consequently, the TIs formed by p-p [53,54], p-d [55–57], and d-d [58,59] orbitals satisfying this condition are candidates to realize SOTSCs from uniform s-wave pairing.

Discussion and conclusion. We have uncovered a different and fundamental mechanism by introducing another concept of a two-particle edge Berry phase to characterize and realize second-order TIs or TSCs. Unlike other basic mechanisms such as the Wilson loop and topological multipole invariants in the bulk, the boundary two-particle Berry phase mechanism provides a fundamental and intuitive principle which facilitates the discovery of high-order topological matter. As

concrete examples of the application, we have predicted a result that the Majorana Kramers pairs of corner modes are realized by directly coupling a type-II TR invariant TI edge to a uniform *s*-wave SC, which stands in sharp contrast to previous proposals. We further predicted the Au/GaAs(111) film as a material candidate for the realization of the SOTSC, and a generic class of candidate materials is also discussed. Our prediction shall inspire further theoretical and experimental studies, including also the extension of the present study to higher dimensions.

Acknowledgments. This work was supported by the National Key R&D Program of China (Grant No. 2021YFA1400900), National Natural Science Foundation of China (No. 11825401 and No. 11921005), and the Strategic Priority Research Program of Chinese Academy of Science (Grant No. XDB28000000).

[1] M. Z. Hasan and C. L. Kane, Rev. Mod. Phys. **82**, 3045 (2010).
[2] X.-L. Qi and S.-C. Zhang, Rev. Mod. Phys. **83**, 1057 (2011).
[3] A. Bansil, H. Lin, and T. Das, Rev. Mod. Phys. **88**, 021004 (2016).
[4] W. A. Benalcazar, B. A. Bernevig, and T. L. Hughes, Science **357**, 61 (2017).
[5] W. A. Benalcazar, B. A. Bernevig, and T. L. Hughes, Phys. Rev. B **96**, 245115 (2017).
[6] J. Langbehn, Y. Peng, L. Trifunovic, F. von Oppen, and P. W. Brouwer, Phys. Rev. Lett. **119**, 246401 (2017).
[7] Z. Song, Z. Fang, and C. Fang, Phys. Rev. Lett. **119**, 246402 (2017).
[8] F. Schindler, A. M. Cook, M. G. Vergniory, Z. Wang, S. S. P. Parkin, B. A. Bernevig, and T. Neupert, Sci. Adv. **4**, eaat0346 (2018).
[9] M. Geier, L. Trifunovic, M. Hoskam, and P. W. Brouwer, Phys. Rev. B **97**, 205135 (2018).
[10] G. van Miert and C. Ortix, Phys. Rev. B **98**, 081110(R) (2018).
[11] X.-L. Sheng, C. Chen, H. Liu, Z. Chen, Z.-M. Yu, Y. X. Zhao, and S. A. Yang, Phys. Rev. Lett. **123**, 256402 (2019).
[12] C. Chen, Z. Song, J.-Z. Zhao, Z. Chen, Z.-M. Yu, X.-L. Sheng, and S. A. Yang, Phys. Rev. Lett. **125**, 056402 (2020).
[13] R. Jackiw and C. Rebbi, Phys. Rev. D **13**, 3398 (1976).
[14] D. Călugăru, V. Juričić, and B. Roy, Phys. Rev. B **99**, 041301(R) (2019).
[15] F. Schindler, J. Appl. Phys. **128**, 221102 (2020).
[16] M. Ezawa, Phys. Rev. B **98**, 045125 (2018).
[17] F. Liu, H. Y. Deng, and K. Wakabayashi, Phys. Rev. Lett. **122**, 086804 (2019).
[18] B. Liu, G. Zhao, Z. Liu, and Z. F. Wang, Nano Lett. **19**, 6492 (2019).
[19] E. Lee, R. Kim, J. Ahn, and B.-J. Yang, npj Quantum Mater. **5**, 1 (2020).
[20] C. Chen, W. Wu, Z.-M. Yu, Z. Chen, Y. X. Zhao, X.-L. Sheng, and S. A. Yang, Phys. Rev. B **104**, 085205 (2021).
[21] Y. Ren, Z. Qiao, and Q. Niu, Phys. Rev. Lett. **124**, 166804 (2020).
[22] F. Liu and K. Wakabayashi, Phys. Rev. Research **3**, 023121 (2021).
[23] B. Liu, L. Xian, H. Mu, G. Zhao, Z. Liu, A. Rubio, and Z. F. Wang, Phys. Rev. Lett. **126**, 066401 (2021).
[24] T. Liu, J. J. He, and F. Nori, Phys. Rev. B **98**, 245413 (2018).
[25] H. Shapourian, Y. Wang, and S. Ryu, Phys. Rev. B **97**, 094508 (2018).
[26] Z. Yan, Phys. Rev. Lett. **123**, 177001 (2019).
[27] X. Zhu, Phys. Rev. Lett. **122**, 236401 (2019).
[28] Z. Wu, Z. Yan, and W. Huang, Phys. Rev. B **99**, 020508(R) (2019).
[29] R.-X. Zhang, W. S. Cole, X. Wu, and S. Das Sarma, Phys. Rev. Lett. **123**, 167001 (2019).
[30] Y. Peng and Y. Xu, Phys. Rev. B **99**, 195431 (2019).
[31] X.-H. Pan, K.-J. Yang, L. Chen, G. Xu, C.-X. Liu, and X. Liu, Phys. Rev. Lett. **123**, 156801 (2019).
[32] B. Roy, Phys. Rev. B **101**, 220506(R) (2020).
[33] Q. Wang, C.-C. Liu, Y.-M. Lu, and F. Zhang, Phys. Rev. Lett. **121**, 186801 (2018).
[34] Z. Yan, F. Song, and Z. Wang, Phys. Rev. Lett. **121**, 096803 (2018).
[35] Y. Volpez, D. Loss, and J. Klinovaja, Phys. Rev. Lett. **122**, 126402 (2019).
[36] C. Zeng, T. D. Stanescu, C. Zhang, V. W. Scarola, and S. Tewari, Phys. Rev. Lett. **123**, 060402 (2019).
[37] K. Laubscher, D. Chughtai, D. Loss, and J. Klinovaja, Phys. Rev. B **102**, 195401 (2020).
[38] X.-J. Liu, C. L. M. Wong, and K. T. Law, Phys. Rev. X **4**, 021018 (2014).
[39] K. Wölms, A. Stern, and K. Flensberg, Phys. Rev. Lett. **113**, 246401 (2014).
[40] K. Wölms, A. Stern, and K. Flensberg, Phys. Rev. B **93**, 045417 (2016).
[41] P. Gao, Y.-P. He, and X.-J. Liu, Phys. Rev. B **94**, 224509 (2016); **95**, 019902(E) (2017).
[42] A. Haim and Y. Oreg, Phys. Rep. **825**, 1 (2019).
[43] C. Knapp, A. Chew, and J. Alicea, Phys. Rev. Lett. **125**, 207002 (2020).
[44] J.-S. Hong, T.-F. J. Poon, L. Zhang, and X.-J. Liu, Phys. Rev. B **105**, 024503 (2022).
[45] Y. Zhang, K. Jiang, F. Zhang, J. Wang, and Z. Wang, Phys. Rev. X **11**, 011041 (2021).
[46] J. Wu, J. Liu, and X.-J. Liu, Phys. Rev. Lett. **113**, 136403 (2014).
[47] L. Fu and C. L. Kane, Phys. Rev. B **79**, 161408(R) (2009).
[48] J. Alicea, Rep. Prog. Phys. **75**, 076501 (2012).
[49] E. Hilner, A. Mikkelsena, J. Eriksson, J. N. Andersen, and E. Lundgren, Appl. Phys. Lett. **89**, 251912 (2006).
[50] Z. F. Wang, K.-H. Jin, and F. Liu, Nat. Commun. **7**, 12746 (2016).
[51] R.-X. Zhang, H.-C. Hsu, and C.-X. Liu, Phys. Rev. B **93**, 235315 (2016).
[52] See Supplemental Material at http://link.aps.org/supplemental/10.1103/PhysRevB.105.L041105 for details on the formalism of two-state Berry phases, the pseudospin analysis for the BHZ and Kane-Mele model, and the derivation of boundary

pseudospin texture of the material candidate, which includes Refs. [12,21,50].

[53] J. J. Zhou, W. Feng, C. C. Liu, S. Guan, and Y. Yao, Nano Lett. **14**, 4767 (2014).

[54] C. Li, K.-H. Jin, S. Zhang, F. Wang, Y. Jia, and F. Liu, Nanoscale **10**, 5496 (2018).

[55] X. Qian, J. Liu, L. Fu, and J. Li, Science **346**, 1344 (2014).

[56] M. Yang and W. M. Liu, Sci. Rep. **4**, 5131 (2014).

[57] B. Huang, K. H. Jin, H. L. Zhuang, L. Zhang, and F. Liu, Phys. Rev. B **93**, 115117 (2016).

[58] H. Weng, A. Ranjbar, Y. Liang, Z. Song, M. Khazaei, S. Yunoki, M. Arai, Y. Kawazoe, Z. Fang, and X. Dai, Phys. Rev. B **92**, 075436 (2015).

[59] C. Si, K. H. Jin, J. Zhou, Z. Sun, and F. Liu, Nano Lett. **16**, 6584 (2016).